Dimesitylketone O −Oxide: Spectroscopic Characterization, Conformation, and Reaction Modes: OH Formation and OH Capture

ARTICLE *in* JOURNAL OF THE AMERICAN CHEMICAL SOCIETY · APRIL 2001

Impact Factor: 12.11 · DOI: 10.1021/ja003533g · Source: PubMed

Dimesitylketone *O*-Oxide: Spectroscopic Characterization, Conformation, and Reaction Modes: OH Formation and OH Capture

Wolfram Sander,*,† Klaus Block,† Wilhelm Kappert,† Andreas Kirschfeld,† Sengodagounder Muthusamy,† Kerstin Schroeder,† Carlos P. Sosa,‡ Elfi Kraka,§ and Dieter Cremer*,§

Contribution from the Lehrstuhl für Organische Chemie II der Ruhr-Universität, D-44780 Bochum, Germany, Cray Inc., 1340 Mendota Heights Road, Mendota, Minnesota 55120, and Department of Theoretical Chemistry, Göteborg University, Reutersgatan 2, S-41320 Göteborg, Sweden

Received September 28, 2000. Revised Manuscript Received December 14, 2000

Abstract: Dimesitylketone *O*-oxide **1b** was synthesized by photolysis of dimesityldiazomethane dissolved in an oxygen saturated CCl_3F solution at 140 K. Conformation and geometry of **1b** were determined by comparing measured NMR chemical shifts with the corresponding chemical shifts calculated at the DFT-IGLO level of theory where it had to be considered that the molecule exists in two enantiomeric forms. Measured and calculated ^1H chemical shifts agree within 0.1 ppm while the calculated ^{13}C shift of the COO carbon (210.6 ppm) differs by only 0.4 ppm from the measured shift of 211.0 ppm. The two mesityl rings are perpendicular to each other and enclose angles of 40 and 57° with the COO plane. The preferred rearrangement process of **1b** is an H migration from one of the *ortho*-methyl groups to the terminal O atom of the COO unit. The calculated activation enthalpy of this process is 12.7 kcal/mol (B3LYP/cc-pVTZ). In contrast, the activation enthalpy for isomerization to dioxirane is 5 kcal/mol higher. In CCl_3F, the activation barrier for the thermal decay was determined to be 13.8 ± 0.2 kcal/mol and in acetonitrile 13.1 ± 0.4 kcal/mol. H migration initiates cleavage of the OO bond and the production of an OH and a benzyl radical. Recombination of the latter in the solvent cage leads to the formation of 2-methylhydroxy-pentamethylbenzophenone, while escape of the OH radical from the solvent cage yields a ketone. These results confirm the possibility of OH production from carbonyl oxides in the solution phase.

1. Introduction

Carbonyl *O*-oxides **1** were proposed as key intermediates in the ozonolysis of alkenes by Criegee et al. more than fifty years ago.[1,2] Although there is ample evidence for such mechanism,[3] a carbonyl oxide **1** has never been observed by direct spectroscopic methods in an ozonolysis reaction. An alternative path to produce **1** is through the oxidation of diazo compounds **2**, either via triplet carbenes, which are rapidly trapped by molecular oxygen $^3O_2$ ("triplet route"),[4−12] or by the reaction of **2** with singlet oxygen $^1O_2$ ("singlet route").[13,14] It was also demonstrated that singlet carbenes and $^3O_2$ produce **1**, although this reaction generally is much slower than the oxidation of triplet carbenes.[15 − 19]

During the last years, lifetimes, photochemistry, IR, and UV−vis spectra have been determined for a large number of carbonyl oxides by combining time-resolved studies in solution at room temperature and matrix isolation at cryogenic temperatures.[4−19] The most characteristic spectroscopic features of **1** are strong and broad absorptions in the visible region around 400 nm, and in the IR the OO stretching vibrations around 900 cm^{-1}.[11,20] In solution, **1** are transient species with lifetimes in the order of ms, while under the conditions of matrix isolation **1** are stable, although extremely sensitive toward visible and UV light irradiation.

† Ruhr-Universität.
‡ Cray Inc.
§ Göteborg University.

(1) Criegee, R.; Wenner, G. *Liebigs Ann. Chem.* **1949**, *564*, 9−15.
(2) Criegee, R. *Angew. Chem.* **1975**, *87*, 765−771; *Angew. Chem., Int. Ed. Engl.* **1975**, *14*.
(3) Kuczkowski, R. L. Ozone and Carbonyl Oxides. In *1,3-Dipolar Cycloaddition Chemistry*; Padwa, A., Ed.; Wiley: London, 1984; Vol. 2, Chapter 11, pp 197−276.
(4) Bartlett, P. D.; Traylor, T. G. *J. Am. Chem. Soc.* **1962**, *84*, 3408−3409.
(5) Sugawara, T.; Iwamura, H.; Hayashi, H.; Sekiguchi, A.; Ando, W.; Liu, M. T. H. *Chem. Lett.* **1983**, 1261−1262.
(6) Werstiuk, N. H.; Casal, H. L.; Scaiano, J. C. *Can. J. Chem.* **1984**, *62*, 2391−2392.
(7) Bell, G. A.; Dunkin, I. R. *J. Chem. Soc., Chem. Commun.* **1983**, 1213−1215.
(8) Dunkin, I. R.; Shields, C. J. *J. Chem. Soc., Chem. Commun.* **1986**, 154−156.
(9) Sander, W. *Angew. Chem.* **1986**, *98*, 255−256; *Angew. Chem., Int. Ed. Engl. 25*, **1986**, 255−257.
(10) Sander, W. W. *J. Org. Chem.* **1989**, *54*, 333−339.
(11) Sander, W. *Angew. Chem.* **1990**, *102*, 362−372; *Angew. Chem., Int. Ed. Engl.* **1990**, *29*, 344−354.
(12) Sander, W. W.; Patyk, A.; Bucher, G. *J. Mol. Struct.* **1990**, *222*, 21−31.
(13) Casal, H. L.; Sugamori, S. E.; Scaiano, J. C. *J. Am. Chem. Soc.* **1984**, *106*, 7623−7624.
(14) Casal, H. L.; Tanner, M.; Werstiuk, N. H.; Scaiano, J. C. *J. Am. Chem. Soc.* **1985**, *107*, 4616−4620.
(15) Ganzer, G. A.; Sheridan, R. S.; Liu, M. T. H. *J. Am. Chem. Soc.* **1986**, *108*, 1517−1520.
(16) Wierlacher, S.; Sander, W.; Liu, M. T. H. *J. Org. Chem.* **1992**, *57*, 1051−1053.
(17) Liu, M. T. H.; Bonneau, R.; Jefford, C. W. *J. Chem. Soc., Chem. Commun.* **1990**, 1482−1483.
(18) Nojima, T.; Ishiguro, K.; Sawaki, Y. *Chem. Lett.* **1995**, 545−546.
(19) Nojima, T.; Ishiguro, K.; Sawaki, Y. *J. Org. Chem.* **1997**, *62*, 6911−6917.
(20) Bucher, G.; Sander, W. *Chem. Ber.* **1992**, *125*, 1851−1859.

10.1021/ja003533g CCC: $20.00
Published on Web 02/23/2001

Scheme 1

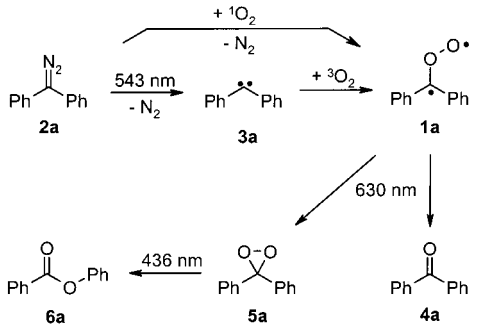

Benzophenone *O*-oxide **1a** is a prototypic carbonyl oxide that has been investigated extensively (Scheme 1). In acetonitrile at room temperature **1a** exhibits an absorption with $\lambda_{max} = 410$ nm,[13,21,22] which in argon at 10 K is slightly red-shifted to 422 nm.[9,10] A very strong IR absorption at 896 cm^{-1} (argon, 10 K) was assigned to the OO stretching vibration.[9,10] Using time-resolved dielectric loss experiments, a dipole moment of 4.0 D was measured for **1a**. This dipole moment is larger than expected for a diradical, but somewhat smaller than the dipole moment calculated for a zwitterion (ca. 5 D). Studies based on photoacoustic calorimetry have reported that the reaction of diphenyldiazomethane **2a** with $^3O_2$ to produce **1a** and N_2 is exothermic by 48 ± 0.8 kcal/mol.[23] The lifetime of **1a** in solution is limited by the dimerization to give 1,2,4,5-tetraphenyltetroxane with a second-order rate constant $k = 1.33 \times 10^7$ M^{-1} s^{-1}.[21] Irradiation of matrix isolated **1a** with red light (630 nm) yields benzophenone **4a** (minor product) and diphenyldioxirane **5a**, which on irradiation with blue light (430 nm) is converted to phenyl benzoate **6a** (Scheme 1).

For the efficient synthesis of carbonyl oxides **1** via the triplet route, the triplet carbene has to have a lifetime that is long enough to guarantee its efficient capture by molecular oxygen. The sterically hindered dimesitylcarbene **3b**[24−28] in solution at room temperature exhibits a lifetime of 160 ms[29] and thus exceeds the lifetime of **3a** by 5 orders of magnitude. Since the oxygenation of **3b** is only 1 order of magnitude slower than that of **3a**, the triplet route should be very efficient for the synthesis of **1b**.

Scaiano et al. have demonstrated using time-resolved spectroscopy that dimesitylketone *O*-oxide **1b** can be generated as a transient species in acetonitrile from dimesityldiazomethane **2b** via the triplet and the singlet route.[21] The absorption maximum of **1b** was found at 390 nm, close to that of **1a**. The decay of **1b** is several orders of magnitude slower than that of **1a** and other related diarylketone oxides, where the decay follows first-order kinetics ($k = 1.85$ s^{-1}). They concluded that **1a** does not dimerize, and an inefficient first-order process, e. g. secondary photolysis by the monitoring beam, becomes the predominant decay mechanism. Recently, we have reported in a short communication the synthesis of **1b** in solution at low temperature. **1b** is the first carbonyl oxide that has been reported to be stable in solution and that has been characterized by NMR spectroscopy under these conditions.[30−32]

Scheme 2

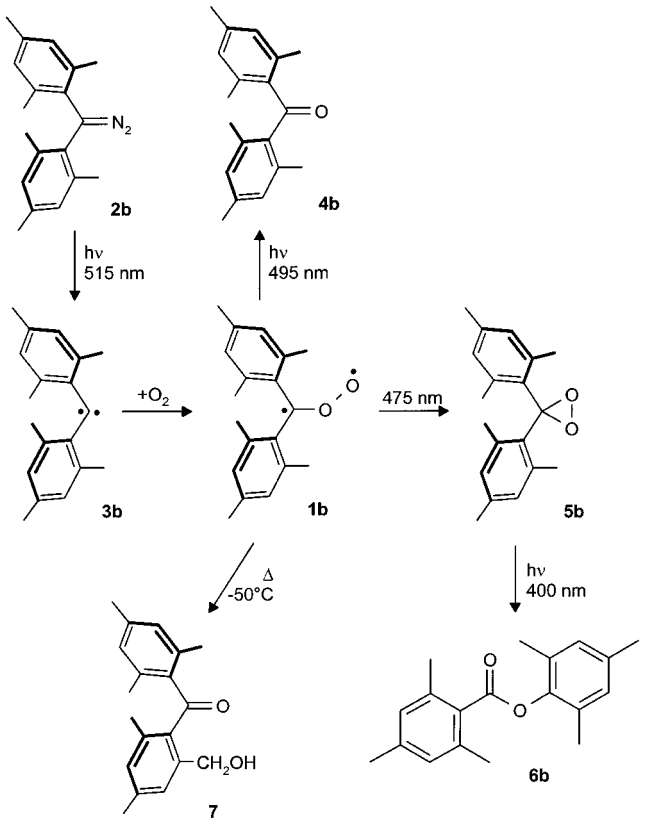

In this work, we describe the synthesis of **1b** as yellow solutions in various solvents, which are stable at dry ice temperature (−78 °C). Utilizing measured and calculated NMR chemical shifts, we explain the experimental NMR spectrum and determine the equilibrium conformation of **1b** in solution. In addition, we investigate rearrangement and decomposition modes of **1b** with a focus on the possibility of OH generation, which has been found an important reaction of carbonyl oxides in the gas phase, but was not observed so far in the solution phase.[33−35]

2. Results and Discussion

2.1 Synthesis of Carbonyl Oxide 1b. The direct visible light photolysis (λ > 515 nm) of diazomethane **2b** in solution, in organic glasses, or in argon matrices results in the formation of the sterically hindered dimesitylcarbene **3b**, which in the presence of $^3O_2$ is efficiently trapped to give dimesitylketone *O*-oxide **1b** (Scheme 2). Since **1b** is photolabile, the yield of **1b** is limited by the slow secondary photochemical rearrange-

(21) Scaiano, J. C.; McGimpsey, W. G.; Casal, H. L. *J. Org. Chem.* **1989**, *54*, 1612−1616.
(22) Girard, M.; Griller, D. *J. Phys. Chem.* **1986**, *90*, 6801−6804.
(23) Hartstock, F. W.; Kanabus-Kaminska, J. M.; Griller, D. *Int. J. Chem. Kinet.* **1989**, *21*, 157−163.
(24) Zimmerman, H. E.; Paskovich, D. H. *J. Am. Chem. Soc.* **1964**, *86*, 2149−2160.
(25) Nazran, A. S.; Gabe, E. J.; LePage, Y.; Northcott, D. J.; Park, J. M.; Griller, D. *J. Am. Chem. Soc.* **1983**, *105*, 2912−2913.
(26) Gilbert, B. C.; Griller, D.; Nazran, A. S. *J. Org. Chem.* **1985**, *50*, 4738−4742.
(27) Nazran, A. S.; Lee, F. L.; Gabe, E. J.; Lepage, Y.; Northcott, D. J.; Park, J. M.; Griller, D. *J. Phys. Chem.* **1984**, *88*, 5251−5254.
(28) Nazran, A. S.; Griller, D. *J. Am. Chem. Soc.* **1984**, *106*, 543−547.
(29) Tomioka, H.; Okada, H.; Watanabe, T.; Banno, K.; Komatsu, K.; Hirai, K. *J. Am. Chem. Soc.* **1997**, *119*, 1582−1593.
(30) Kirschfeld, A.; Muthusamy, S.; Sander, W. *Angew. Chem.* **1994**, *106*, 2261−2263; *Angew. Chem., Int. Ed. Engl. 33*, **1994**, 2212.
(31) Sander, W.; Kirschfeld, A.; Kappert, W.; Muthusamy, S.; Kiselewsky, M. *J. Am. Chem. Soc.* **1996**, *118*, 6508−6509.
(32) Sander, W.; Schroeder, K.; Muthusamy, S.; Kirschfeld, A.; Kappert, W.; Boese, R.; Kraka, E.; Sosa, C.; Cremer, D. *J. Am. Chem. Soc.* **1997**, *119*, 7265−7270.
(33) Gutbrod, R.; Schindler, R. N.; Kraka, E.; Cremer, D. *Chem. Phys. Lett.* **1996**, *252*, 221−229.
(34) Gutbrod, R.; Kraka, E.; Schindler, R. N.; Cremer, D. *J. Am. Chem. Soc.* **1997**, *119*, 7330−7342.
(35) Olzmann, M.; Kraka, E.; Cremer, D.; Gutbrod, R.; Andersson, S. *J. Phys. Chem. A* **1997**, *101*, 9421−9429.

ment to dioxirane **5b** during the 515 nm irradiation of the diazo precursor. In addition, thermal rearrangements and intermolecular reactions with the solvent decrease the yield of **1b**. Thus, short irradiation times, low temperatures, and an inert solvent toward both carbene **3b** and carbonyl oxide **1b** are necessary to obtain high yields of **1b**. Initially, the photochemical generation of **1b** from **2b** was carried out in an oxygen saturated 1:1 mixture of CCl_3F and $(CF_2Br)_2$, which forms a transparent glass at 77 K.[36] After irradiating the glass at 77 K for several hours, **1b** was produced as a intensively yellow compound (λ_{max} = 398 nm) with 20−25% yield (in the glass determined by UV−vis spectroscopy, in solution by ^{1}H NMR, see below). After melting the glass at 140 K, the yellow solution remains stable at this temperature for many hours.

A similar yield for **1b** is obtained after photolysis of a stirred, oxygen-saturated solution of **2b** in CCl_3F at 140 K. The triplet route (direct photolysis of **2b**) is not limited to perhalogenated solvents: **1b** can also be synthesized by photolysis of oxygen-saturated solutions of **2b** in a 1:4 mixture of pentane/toluene at 160 K or THF at 173 K.

Alternatively, carbonyl oxide **1b** can be synthesized via reaction of diazomethane **2b** with singlet oxygen (singlet route). The advantage of the singlet route is that the sensitizer rather than **2b** is excited, and thus secondary photolysis of **1b** is reduced by irradiation at longer wavelengths. Furthermore, since carbene **3b** is not formed as an intermediate, reactions of **3b** with the solvent are avoided.

Also, carbonyl oxide **1b** was synthesized by the oxidation of **2b** with $^1O_2$ at 173 K in a 1:4 mixture of pentane/toluene with C_{60} as sensitizer, or in THF with rose bengal as sensitizer (λ > 570 nm irradiation in both cases). The disadvantage of the latter combination of solvent/sensitizer is the rapid bleaching of rose bengal under these conditions. The best results were obtained in CCl_3F at 220 K with a 2.5×10^{-3} molar solution of **2b** and 5,10,15,20-tetrakis(pentafluorophenyl)-21*H*,23*H*-porphin as sensitizer (λ > 570 nm irradiation).

2.2 Spectroscopic Characterization of 1b. In CCl_3F, THF, or solid argon, carbonyl oxide **1b** exhibits a strong UV−vis absorption with a maximum at 396 ± 2 nm. In pentane or pentane/toluene the maximum is blue-shifted to 338 nm. Since the effect of the polarity of the solvent (argon vs THF) on the absorption maximum is very small, the large shift in pentane presumably is caused by aggregation of the highly polar **1b** in the unpolar pentane. During the reaction of **2b** with $^1O_2$ in THF an isosbestic point at 470 nm is observed, which suggests that **1b** is formed quantitatively under these conditions. From that an extinction coefficient of $\epsilon = 4400$ l cm^{-1} mol^{-1} is estimated, in qualitative agreement with our earlier semiempirical calculations of the UV−vis spectrum of **1a** (CNDO/S: λ_{max} = 455 nm, ϵ = 6900).[37] The IR spectrum of **1b** (matrix-isolated in argon at 10 K) shows an intense band at 877 cm^{-1}.[32] This band is assigned to the OO stretching vibration (**1a**: 896 cm^{-1}),[10] which is red-shifted by 31 cm^{-1} on ^{18}O labeling (**1a**: 35 cm^{-1} ^{18}O isotopic shift). The band position and the isotopic shift are highly characteristic of carbonyl oxides.[11,38]

The NMR spectra for **1b** were recorded by generating the carbonyl oxide in $CCl_3F/(CBrF_2)_2$ at 77 K, melting the organic glass at 165 K, and then transferring the yellow solution into an NMR probe pre-cooled to 203 K. ^{13}C-**2b** (99% ^{13}C-label at the diazo position) was used in the NMR experiments which allowed to record both ^{13}C- and ^{1}H NMR spectra in the same experiment. The ^{13}C NMR spectrum of the yellow solution exhibits a signal for nonreacted ^{13}C-**2b** at δ = 58.0, a weak signal of dimesitylketone ^{13}C-**4b** at δ = 202.8, and a signal of a new compound at δ = 211.1. After warming to room temperature and cooling back to 203 K a colorless solution is obtained in which the new compound has completely disappeared, and more ketone **4b** and an additional compound with a signal at δ = 204.7 is formed. The latter could be separated by preparative scale HPLC and spectroscopically characterized as benzyl alcohol **7** (Scheme 2). The fact that the yellow color of **1b** simultaneously vanishes with the signal at δ = 211.1 suggests that the color as well as the signal corresponds to **1b**. This indicates that the chemical shift of the carbonyl carbon of **1b** appears in the carbonyl region only 6.4 ppm downfield of that of ketone **4b**.

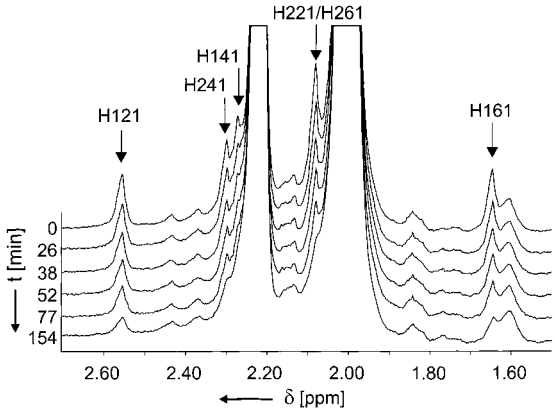

Figure 1. Aliphatic region of the ^{1}H NMR spectrum of **1b** in $CCl_3F/(CBrF_2)$ at 233 K. Peaks marked by an arrow decrease with a first-order kinetics and are assigned to the methyl groups of **1b**. The large peaks are due to unreacted diazo compound **2b**.

The ^{1}H NMR spectrum of **1b** could also be recorded in a Freon mixture at 203 K (Figure 1). The ^{1}H chemical shifts assignments in the yellow solution are complicated due to signal overlap between **1b**, **2b**, and **4b**. On the basis of the thermal lability of the carbonyl oxide, seven signals (all singlets which disappeared on warming the solution) are assigned to **1b**: 6.95 (1 H), 6.82 (2 H), 2.53 (3 H), 2.28 (3 H), 2.25 (3 H), 2.05 (6 H), and 1.61 (3 H). In this group, there are only two signals in the region of aromatic protons and five signals for the methyl groups. To identify important signals that might overlap with signals resulting from remaining starting material or byproducts, a ^{1}H COSY experiment was performed (Figure 2). A "missing" aryl proton is located at δ = 6.7. In addition, the long range ^{1}H,^{1}H couplings were used to identify all proton signals in the two mesityl rings A and B (Scheme 3, Figure 3).

For ring A we identify three distinct signals, namely one signal corresponding to six hydrogen atoms for the *ortho*-methyl groups H121 and H161, one signal corresponding to two hydrogen atoms for the two *meta*-aryl hydrogen atoms H13 and H15, and one signal for the *para*-positioned methyl group (Scheme 3). Five signals in the NMR proton spectrum can be assigned to ring B. There are two signals for the two *ortho*-methyl groups H221 and H261 and an additional signal for the *para*-methyl group H241 (Table 1). The two aryl protons H23 and H25 also lead to two signals, which clearly demonstrates that in ring B all methyl groups and the aryl protons are nonequivalent.

The NMR experiment does not clarify whether the observed signal patterns correspond to stationary conformations C_s I

(36) Kappert, W.; Sander, W.; Landgrafe, C. *Liebigs Ann.* **1997**, 2519−2524.

(37) Cremer, D.; Schmidt, T.; Sander, W.; Bischof, P. *J. Org. Chem.* **1989**, *54*, 2515−2522.

(38) Sander, W.; Bucher, G.; Wierlacher, S. *Chem. Rev.* **1993**, *93*, 1583−1621.

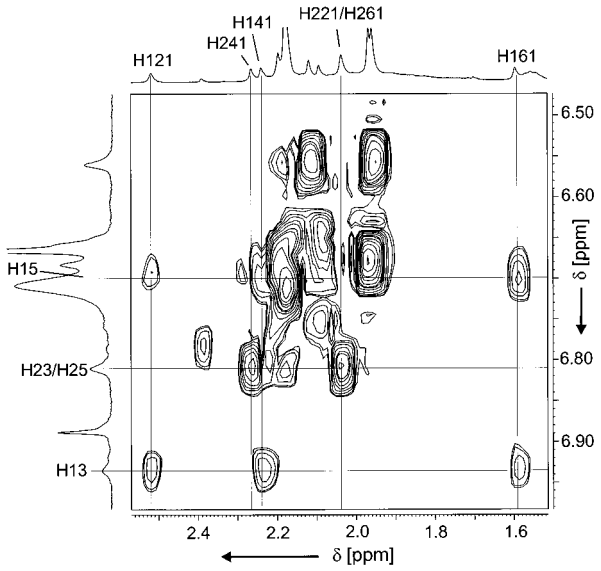

Figure 2. H,H correlation via long-range coupling of **1b** in $CCl_3F/(CF_2Br)_2$ at 203 K.

Scheme 3

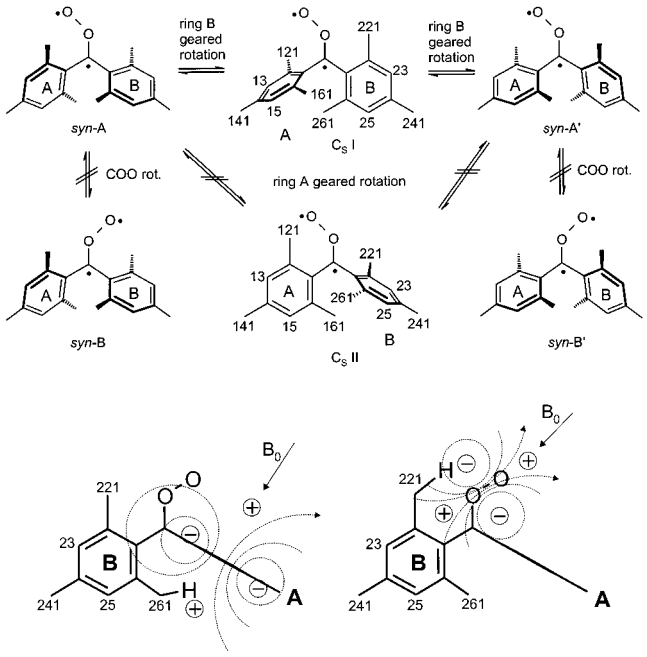

Figure 3. Anisotropic magnetic fields induced by mesityl ring B and the COO group mainly influence the *ortho*-methyl groups of ring A. H161 is shifted to high field while H121 is shifted to low field.

(Scheme 3; ring A has 3, ring B 5 proton signals) or C_s II (Scheme 3; ring A has 5, ring B 3 proton signals) or whether they correspond to rapidly equilibrating enantiomeric structures (*syn*-A and *syn*-A′ or *syn*-B and *syn*-B′) with time-averaged C_s symmetry (C_s-symmetrical conformer as TS). The latter process would involve geared librations of the two rings (caused by the steric interactions between the *ortho* methyl groups of the rings A and B), which in the time average also would yield the observed signal patterns. There is the possibility of a B,A libration (TS: C_s I) or an A,B libration (TS: C_s II, Scheme 3), where the first ring drives the movement of the second ring.

The NMR experiment clearly excludes rapid full rotations of mesityl rings A and B at 203 K. This could occur only in a geared fashion, thus reducing the number of signals from five to three for ring B. Also, the *syn*-A−*syn*-B isomerization, either via COO rotation or inversion, cannot occur, because it would lead to a further simplification of the NMR spectrum. Finally, we note that nonequilibrating enantiomers would lead to five rather than three signals for ring A and, therefore, can also be excluded.

Table 1. Experimental and Calculated NMR Spectroscopic Data of Dimesitylketone Oxide **1b** Compared to Dimesitylsulfine **8**

	1b			**8**[a]	
assignment	$CCl_3F/(CF_2Br)_2$ 203 K	**1b** DFT-IGLO[b]	Δ	$CDCl_3$ 233 K	Δ
C	211.1	210.6	−0.5	188.5	
H13	6.95	6.88	−0.07	7.00	0.05
H15	∼6.7	6.55	−0.15	6.82	0.12
H121	2.53	2.43	−0.1	2.67	0.14
H141	2.25	2.32	0.09	2.27	0.02
H161	1.61	1.48	−0.13	1.79	0.18
H23/H25		6.72, 6.50			
Average	6.82	6.61	−0.21	6.91	0.09
H221/H261		2.48, 1.66			
average	2.05	2.07	0.02	2.17	0.12
H241	2.28	2.34	0.04	2.26	0.02

[a] Reference 36. [b] DFT-IGLO calculations at BPW91/[5s4p1d/3s1p], shifts are given with regard to TMS. Calculated shieldings are: ^{13}C: 186.07; ^{1}H: 31:18 ppm (see also refs 40 and 41).

Calculations (supporting an analysis of steric interactions between the terminal O atom and the methyl group 121 by inspection) show that a conformer such as C_s II (Scheme 3) has little stability (15.6 kcal/mol relative to the energy of **1b** at B3LYP/6-31G(d); $\Delta\Delta H_f^0(298) = 15.1$ kcal/mol), and therefore, any geared libration passing through C_s II as TS will be very slow on the NMR time scale. Conformer C_s II and the associated libration process can therefore be excluded to be responsible for the measured NMR pattern. It remains to consider either C_s I or the geared libration *syn*-A to *syn*-A′ to be responsible for the NMR spectrum.

A comparison of the NMR spectra for **1b** and for its stable homologue dimesitylsulfine **8** reveals many similarities between these two compounds (Table 1). Sulfine **8** was structurally characterized by X-ray analysis and NMR spectroscopy using lanthanide shift reagents.[36] In the crystalline form, **8** shows the expected chiral structure with the two mesityl rings rotated by approximately 60° (with respect to the plane defined by the CSO group). In solution an activation barrier of 14 kcal/mol was determined for the geared ring B rotation. The activation barrier for the ring A libration in **8** was recently determined by Lunazzi et al. to be only 5.9 kcal/mol.[39] The latter process results in the time-averaged C_s symmetrical structure of **8** determined by NMR spectroscopy even at low temperature. We calculate that the rotation of ring B in **1b** requires an energy of only 3.3 kcal/mol ($\Delta\Delta H_f^0(298) = 3.0$ kcal/mol at B3LYP/6-31G(d)) in line with the measured activation barrier in **8**. In this connection one has to consider that the COO group is not as bulky as the CSO group, while on the other hand, COO is more rigid than CSO against angle widening. The latter point explains that the barrier of rotation for ring A is 15.6 kcal/mol in the case of **1b** and 14 kcal/mol in the case of **8**.

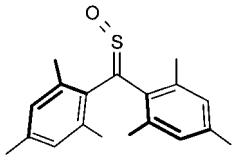

8

(39) Lunazzi, L. Private communication.

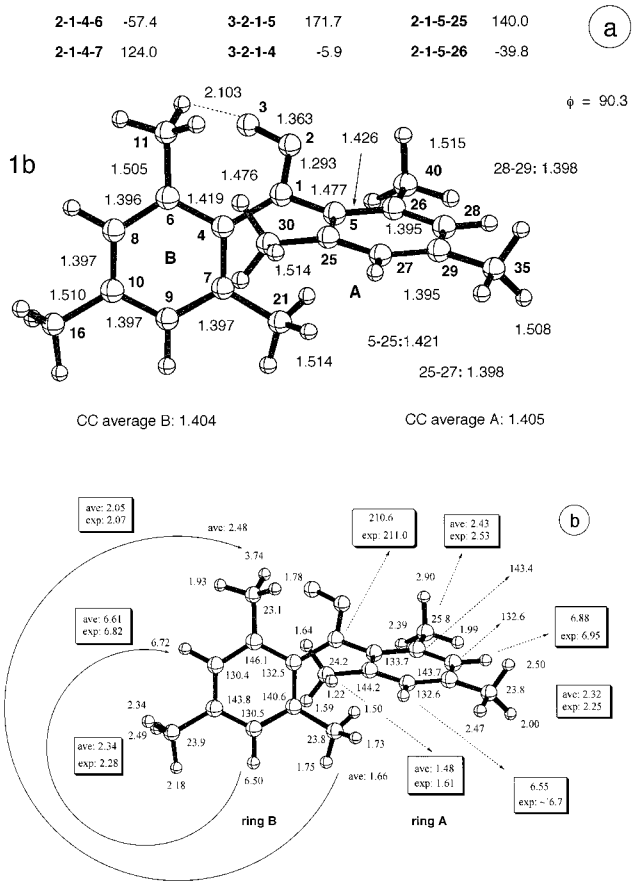

Figure 4. (a) B3LYP/6-31G(d) geometry of carbonyl oxide **1b**. Thin dashed lines indicate nonbonded interactions. For a definition of angle ϕ, see text. Distances and angles are given in Å and deg, respectively. (b) Comparison of measured and calculated NMR chemical shifts. Symbols ave and exp denote averaged (over the three protons of a methyl group or in case of ring B over equivalent protons as indicated by the arrows) and experimental chemical shifts in ppm.

All ^{1}H chemical shifts in **8** are slightly shifted downfield compared to the chemical shifts in **1b**, with the largest deviation being less than 0.2 ppm. It is therefore safe to assume that the structures **1b** and **8** in solution are very similar.

2.3 Quantum Chemical Description of Structure and NMR Chemical Shifts. The equilibrium conformation and NMR chemical shifts of **1b** were determined on the basis of DFT-B3LYP/6-31G(d) calculations. Carbonyl oxide **1b** exists in two enantiomeric forms (*syn*-A, *syn*-A′), one of which is shown in Figure 4a, while the second is obtained by reverting the signs of the dihedral angles given in the heading of Figure 4a. The calculated structure of **1b** is similar to that of **8** determined by X-ray crystallography,[36] that reveals the close similarity between these two compounds. In the minimum conformation of **1b** ring A is rotated by 40° and ring B by 57° (Figure 4a) in opposite directions out of the CXO plane[40] while the crystal structure of **8** gave rotations of 58° and 55°, respectively.[36] The two ring planes (defined by their mean planes) of **1b** enclose an angle of exactly 90°.

The NMR signals were assigned using the calculated equilibrium conformation (Figure 4a) and the geared equilibration process discussed in section 2.2. The latter guarantees that both enantiomers are equally populated under experimental conditions and that the NMR signals recorded are averages of the signals of the individual enantiomers. This conclusion is nicely confirmed by comparison of the experimental NMR data with the results of the IGLO-DFT calculations[40] (Table 1, Figure 4b). According to these calculations, the chemical shift of the carbonyl carbon of **1b** is predicted at 210.6 ppm, in excellent agreement with the experimental value of 211.0 ppm. After averaging the calculated proton shifts, as required by the existence of two enantiomers in solution, the calculated and measured ^{1}H NMR chemical shifts of **1b** agree within a standard deviation of 0.04 ppm (largest deviation 0.21 ppm, Table 1).[41,40]

Interestingly, the chemical shifts of the two *ortho*-methyl groups H221 and H261 of ring B in **1a** are split by almost 1 ppm. By comparison with the calculated chemical shifts, H261 is assigned to the methyl group of ring B, which is located anti relative to the terminal O atom of the COO group (Scheme 3, structure C_s I). This group is located beneath ring A, shielded by the anisotropic magnetic field of this ring, and thus shifted to high field (Figure 3). Methyl group H221, on the other hand, although further apart from ring A, is deshielded. In addition, the COO group might induce an anisotropic field (comparable to the sulfine group)[42,43] which should increase the low-field shift of H221.

A description of **1b** with the help of ^{13}C chemical shifts is of little use, because the signals of the two mesityl rings strongly overlap as indicated by the calculated chemical shifts given in Figure 4b. In any case, the agreement between calculated and measured NMR chemical shifts discussed above indicates that the calculated geometry represents a reliable model of the true equilibrium geometry in the sense of the DFT-NMR-IGLO method applied in similar cases before.[44,45]

2.4 Thermal Decay of 1b. The yield of **1b** produced in $CCl_3F/(CF_2Br)_2$ by $\lambda > 515$ nm irradiation at 77 K is up to 22% (based on the consumption of **2b**, determined by ^{1}H NMR in solution at 203 K), while the amount of ketone **4b** formed as byproduct is less than 5% in a typical experiment. Alcohol **7** and dioxirane **5b** are not observed under these conditions. Warming to room temperature results in bleaching of the yellow color, disappearance of all signals assigned to **1b**, and formation of ketone **4b** and alcohol **7** in a 1:9 ratio. The ratio of **4b**/**7** depends on the solvent and on the temperature as well. This will be discussed in Section 2.6.

Visible light irradiation ($\lambda > 470$ nm) of the yellow solution of **1b** at low-temperature decolorizes the solution within a few seconds. The main photoproduct is dioxirane **5b**, minor products are ketone **4b** and ester **6b** (ration of **5b**: **4b**: **6b** = 5:3:2). This clearly demonstrates that alcohol **7** and dioxirane **5b** are the principal thermal and photochemical products. On the other hand, ketone **4b**, the product of oxygen loss, is a minor product in both processes.

The kinetics of the thermal decay of carbonyl oxide **1b** was determined in three different solvents, namely CCl_3F, acetonitrile, and hexane. **1b** was generated at temperatures between 210 and 295 K by irradiation of a 2.5×10^{-5} m solution of **2b**

(40) Kraka, E.; Sosa, C. P.; Cremer, D. *Chem. Phys. Lett*. **1996**, *260*, 43−50.

(41) We note that in ref 40 an erroneous assignment of experimental to calculated ^{1}H NMR chemical shifts is reported because the measured data used there were incomplete and the averaging of two enantiomers was not considered.

(42) Tangerman, A.; Zwanenburg, B. *Org. Magn. Reson*. **1977**, *9*, 695−698.

(43) Tangerman, A.; Zwanenburg, B. *J. Chem. Soc., Perkin Trans. 2* **1975**, 352−361.

(44) Cremer, D.; Olsson, L.; Reichel, F.; Kraka, E. *Isr. J. Chem*. **1993**, *33*, 369−385.

(45) Ottosson, C. H.; Kraka, E.; Cremer, D. Pauling's Legacy: Modern Modelling of the Chemical Bonding. In *Theoretical and Computational Chemistry*; Orville-Thomas, W. J., Maksic, Z., Eds.; Elsevier: Amsterdam, 1999; Vol. 6, pp 231−301.

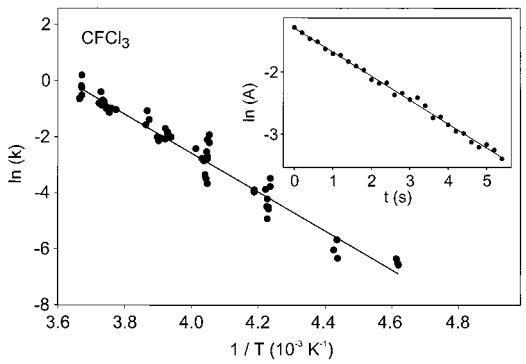

Figure 5. Arrhenius plot for the thermal decay of carbonyl oxide **1b** in CCl_3F. Inset: Thermal decay at 267 K showing first-order kinetics. First-order kinetics is observed at all temperatures.

with the 515 nm light of a pulsed laser. The decay was monitored by UV−vis spectroscopy at a constant temperature until the solution was completely bleached. First-order kinetics was observed at all temperatures. Arrhenius parameters of $E_a = 13.8 \pm 0.2$ kcal/mol and $\log A = 9 \pm 0.6 \times 10^{10}$ were determined by using the temperature dependence of the decay rates in CCl_3F (Figure 5). (By ^{1}H NMR basically the same rates are obtained, however, due to larger errors in the integration of the NMR signals and larger uncertainties in determining the temperature of the sample only the UV−vis data were used to determine the activation parameters). In acetonitrile, a slightly smaller activation barrier (13.1 ± 0.4 kcal/mol) was obtained.

2.5 Mechanism of the Formation of Alcohol 7. In view of the size of the mesityl compounds investigated in this work, quantum chemical calculations were limited by the fact that even with a VDZ+P basis set more than 400 basis functions are needed, which excludes CCSD(T) and other high-level methods because of cost considerations. In recent work by Cremer and co-workers,[33−35,46] it was demonstrated that DFT with the hybrid functional B3LYP[47,48] leads to reliable descriptions of carbonyl oxides close to CCSD(T) quality. For this reason, the various rearrangement modes of **1b** were investigated at the B3LYP level employing the 6-31G(d) basis set[49] (359 basis functions). For each stationary point along the reaction path the geometry was optimized and all vibrational frequencies were calculated. Then, the relative energies were checked by single point calculations at B3LYP/6-31G(d) geometries employing Dunning's cc-pVTZ basis set,[50] which corresponds to a (11s6p3d2f/6s3p2d) [5s4p3d1f/4s3p2d] contraction and implies calculations with 938 basis functions in the case of **1b**. These calculations confirmed the necessity of including f-type polarization functions when describing peroxides.[51]

Previous work[33−35] revealed that carbonyl oxides can rearrange in the gas phase via intramolecular H migration (from a syn positioned methyl or alkyl group to the terminal O atom) to form a hydroperoxyalkene without any biradical character, which then splits off an OH radical and stabilizes as a ketone (Scheme 4, path B). Such a reaction was found to be faster than the isomerization to dioxirane (Scheme 4, path A) and responsible for OH production in the gas phase.[35]

Scheme 4

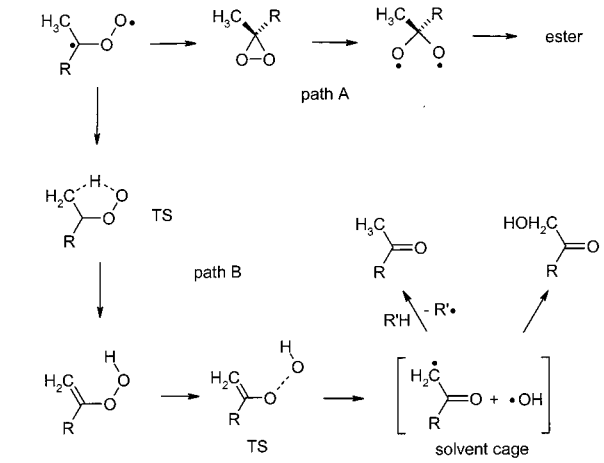

Scheme 5

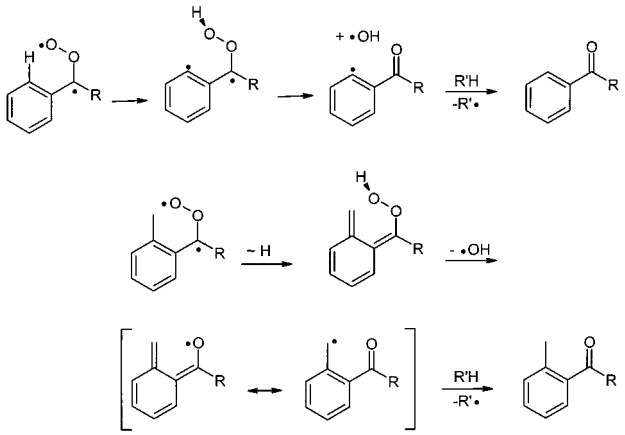

So far, OH formation has not been observed in solution where radical production is more difficult to investigate. Also, it has been considered as unlike possibility in the cases of aryl-substituted carbonyl oxides because this would lead to an intermediate σ,π-biradical with limited possibilities for stabilization (Scheme 5) and a relatively high energy. However, the formation of alcohol **7** suggests reconsidering the possibility of OH formation in the case of a mesityl substituent. Actually, the *ortho*-methyl groups give the mesityl substituent some alkyl character. By H migration, a closed-shell molecule with an *ortho*-quinodimethane structure can be formed (see Scheme 5), which resembles the hydroperoxyalkene formed in the case of *syn*-alkylcarbonyl oxide. On the other hand, formation of a hydroperoxy *ortho*-quinodimethane seems to lead to a (partial) loss of the benzene resonance energy, which would make H migration a relatively high-energy process.

We investigated the alcohol formation at the B3LYP/cc-pVTZ level and found that it follows the mechanism of OH production observed for carbonyl oxides in the gas phase[33−35] (see Table 2, Figure 6, and Figure 7). A number of interesting conclusions can be drawn from the calculations.

(1) H migration involves TS **9** (Figures 6a and 7), which is just 12.7 kcal/mol ($\Delta\Delta H_f^0(298)$ value, Table 2) above the enthalpy of the ground state of **1b** and, by this, energetically more favorable than the TS of the dioxirane formation (18.4 kcal/mol). The relatively low activation enthalpy (dimethyl carbonyl oxide, H migration: 14.4 kcal/mol; dioxirane formation: 21.4 kcal/mol[33]) is a consequence of two important structural factors. (a) In carbonyl oxide **1b**, one of the *o*-methyl hydrogen atoms is already close to the terminal O atoms (Figure

(46) Cremer, D.; Kraka, E.; Szalay, P. G. *Chem. Phys. Lett.* **1998**, *292*, 97−109.
(47) Becke, A. *J. Chem. Phys.* **1993**, *98*, 5648−5652.
(48) Stephens, P. J.; Devlin, F. J.; Chabalowski, C. F.; Frisch, M. J. *J. Phys. Chem.* **1994**, *98*, 11623−11627.
(49) Hariharan, P. C.; Pople, J. A. *Chem. Phys. Lett.* **1972**, *16*, 217.
(50) H., T.; Dunning, J. *J. Chem. Phys.* **1989**, *90*, 1007−1023.
(51) Kraka, E.; Konkoli, Z.; Cremer, D.; Fowler, J.; F., H.; Schaefer, I. *J. Am. Chem. Soc.* **1996**, *118*, 10595−10608.

Table 2. B3LYP/cc-pVTZ Energies and Enthalpies Calculated for the Rearrangement of **1b** to Alcohol **7**[a]

molecule	*E*, Δ*E* 6-31G(d)	cc-pVTZ	ZPE 6-31G(d)	ΔΔH_f°(298) cc-pVTZ	*S* 6-31G(d)	Δ*G*(298) cc-pVTZ	N_{imag}	*μ* 6-31G(d)
1b	−887.60560	−887.91413	226.7	0	151.9	0	0	4.96
9, **TS**	17.9	15.7	223.9	12.7	149.6	13.4	1	3.77
10	14.0	9.9	226.4	9.9	152.8	9.6	0	2.13
11, **TS**	18.5	13.5	224.7	12.1	156.2	10.8	1	4.08
12 + **OH**[b]	6.8	0.4	216.3	−2.9	195.3	−15.9	0	3.51
7	−79.8	−83.4	228.6	−81.2	156.6	−82.6	0	4.89
4b + **O(¹D)**[c]	59.2	58.4	224.8	57.9	188.1	47.1	0	2.71

[a] Absolute energy *E* in hartree, relative energies Δ*E*, enthalpies ΔΔH_f°, free enthalpies Δ*G*, and zero point energies ZPE in kcal/mol, entropies *S* in entropy units, dipole moments *μ* in Debye. N_{imag} gives the number of imaginary frequencies. [b] The energy of OH (6-31G(d): −75.71631; cc-pVTZ: −75.72345 hartree) was added. [c] The energy of O(¹D) (6-31G(d): −74.98827; cc-pVTZ: −75.01951 hartree) was added.

4a: 2.103 Å), which makes this H atom prone to migration to the terminal O atom; (b) in the TS **9,** only a small part of the resonance energy of ring B seems to be lost as indicated by the calculated geometry (Figure 6a): bond C4C6 is elongated to 1.458 Å (1.419 Å in **1b**) while bonds C6C11 and C1C4 are shortened (1.417 and 1.415 Å; **1b**: 1.505 and 1.476 Å). Noteworthy is also that the H approaches the terminal O atom much closer in TS **9** (CH = 1.430; HO = 1.169 Å) than in the H migration TS of an alkylcarbonyl oxide (dimethylcarbonyl oxide: CH = 1.345; HO = 1.344 Å).[33]

(2) An intermediate hydroperoxide of an *ortho*-quinodimethane (**10**) is generated as the product of the H migration, which is 9.9 kcal/mol (Table 2) less stable than **1b**. The average CC bond length of ring B is elongated to 1.430 Å (**1b**: 1.404 Å) and the alternation of bonds as measured by the standard deviation from the average CC bond length is increased to 0.057 Å (**1b**: 0.010 Å). Because of the *ortho*-quinodimethane structure, ring B has to adjust more to the plane defined by C2C1C4 (back-rotation by 34°, Figures 2a and 6b), a process which is (partially) followed by ring A (rotation by 22°) so that the angle between the ring planes reduces from 90 (**1b**) to 85° (Table 3). The destabilization of ring B is partially compensated by H bond-type interactions between C11 and the HOO group.

(3) Cleavage of the OO bond requires just 2.2 kcal/mol (ΔΔH_f^0(298) = 12.1 kcal/mol relative to **1b**, Table 2, Figure 7) and leads to a TS (**11**) that is slightly lower than that of the H migration step. Hence, the latter is the rate determining step and in view of the small thermodynamic and kinetic stability of intermediate **10** there is little chance to isolate **10** and to measure the kinetics of the OO cleavage.

Dissociation reactions normally proceed without a TS along a Morse-type potential. However, in the present case, dissociation is accompanied by strong electronic changes stabilizing the molecule. The CC bonds in ring A become on the average shorter because the *ortho*-quinodimethane structure is changed to that of a benzyl radical with an α-keto group thus regaining a larger part of the resonance energy of a phenyl ring.

(4) The benzyl radical **12** and OH formed in the OO dissociation reaction are of similar stability than **1b** (Δ*E* = 0.4, ΔΔH_f^0(298) = −2.9 kcal/mol, Table 2, Figure 7). Radical **12** is stabilized by (a) the formation of the CO double bond of the keto group and (b) benzyl conjugation (average CC bond for A: 1.412 Å, Table 3, Figure 6d), both being not possible in hydroperoxide **10**.

In the gas phase, reaction path B (Scheme 4) should exclusively lead to ketone **12**, which can stabilize by abstracting a H atom from another molecule. TS searches for a reaction that leads to a direct OH transfer to C11 were unsuccessful.

(5) In solution phase, **1b** will be strongly solvated as suggested by the calculated dipole moment (*μ* = 5 D, Table 2). H migration will occur inside the solvent cage and the activation enthalpy will partially depend on the degree of solvation. We calculate that in TS **9** *μ* is reduced to 3.8 D thus suggesting a decrease in solvation and, by this, an increase in the activation enthalpy.

In any case, OH radical and benzyl radical **12** are formed and captured in a solvent cage where their lifetime in the cage will depend on the dielectric constant of the solvent, its H donor ability, and the temperature of the solution. The longer the OH radical remains in the solvent cage, the larger becomes the possibility of forming the alcohol **7** by radical−radical recombination in a strongly exothermic reaction (ΔΔH_f^0(298) = −81 kcal/mol, Table 2). This is in line with the formation of a new CO single bond and the recovery of the complete resonance energy of ring A (average CC bond length: 1.404 Å and *σ* = 0.010 Å due to low bond alternation, Table 3).

We note that the mechanism suggested by the DFT calculation leads to an activation enthalpy of 12.7 kcal/mol in excellent agreement with the corresponding experimental value. Since the calculations suggest an unimolecular reaction mechanism for the rearrangement of **1b**, the Arrhenius activation energy of 13.8 ± 0.2 kcal/mol in CCl_3F corresponds to an activation enthalpy of 13.2 ± 0.2 kcal/mol and that of 13.1 ± 0.4 kcal/mol in acetonitrile to 12.5 ± 0.3 kcal/mol. Considering that the calculated value will slightly raise in solution because of the reasons discussed above deviations between theory and experiment are smaller than the experimental error of 0.2−0.4 kcal/mol.

2.6 Solvent Dependence of the Formation of Alcohol 7. The relative yields of the thermal products alcohol **7** and ketone **4b** (Scheme 2) proved to be dependent on both the solvent and the temperature of the thermal decay of **1b** (Figure 8). In CCl_3F, the ratio **7**: **4b** increases with temperature from 0.6:1 at 212 K to 2.5:1 at 295 K (a 1:1 ratio is found at about 230 K). In acetonitrile, just the opposite temperature dependence is observed. At 234 K the ratio of **7**: **4b** is 1.3:1 and at 267 K 0.1:1. Hexane shows a very peculiar behavior with the relative yield of **7** increasing with temperature at low temperatures (as in CCl_3F), but above 240 K the relative yield of **7** is again decreasing with rising temperature (as in CH_3CN).

The measured ratios [alcohol]/[ketone] can be analyzed on the background of the rearrangement mechanisms of **1b** discussed in Section 2.5, where we assume that both alcohol **7** and ketone **4b** are produced via path B. During the thermal decay of **2b**, dioxirane **5b** and ester **6** are not formed, and, therefore, the production of any ketone **4b** via path A (Scheme 4) can be excluded. An alternative mechanism is the O transfer from **1b** to unreacted carbene. In addition, the decomposition of **1b** into ketone **4b** + O(¹D) and the insertion of the latter into the CH bond of an *ortho*-methyl group is possible. However, the O−O cleavage is endothermic by 58 kcal/mol

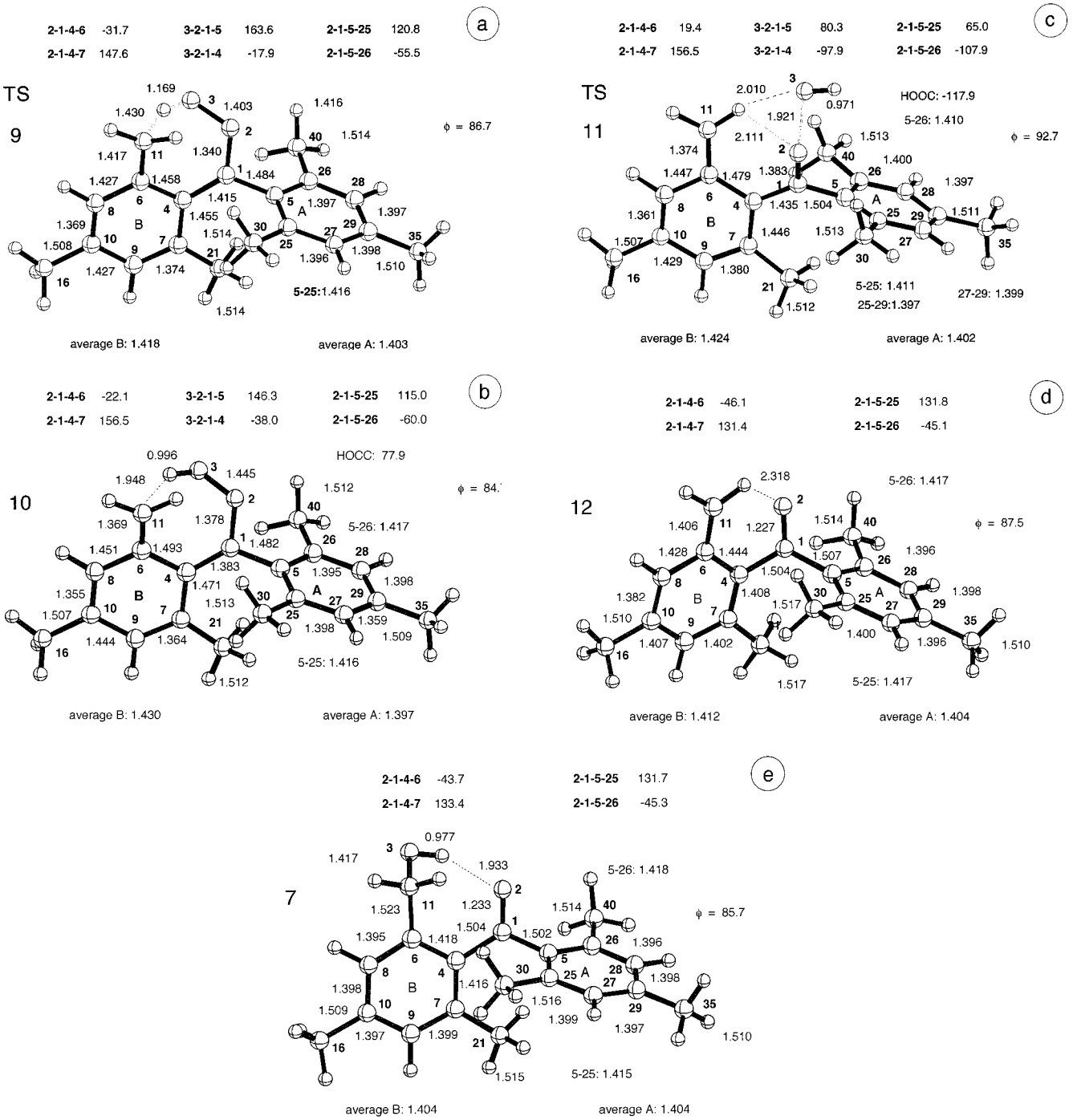

Figure 6. Calculated geometries of carbonyl oxide TS **9** (a), hydroperoxide **10** (b), TS **11** (c), radical **12** (d), and alcohol **7** (e). Distances in Å and angles in deg. Thin dashed lines indicate nonbonded interactions, thick dashed lines breaking or forming bonds in a TS. For a definition of angle ϕ, see text.

(Table 2), which excludes this mechanism for the formation of ketone or alcohol. It is also unreasonable to assume a second transition state of somewhat higher energy than TS **11**, in which the OH group is shifted toward C11, so that alcohol **7** is formed in a concerted reaction from **10**. It is more likely that the fate of the reaction is determined on the stage of **12** + OH both embedded in a solvent cage.

The relative yields of alcohol **7** versus ketone **4b** formed via path B depends on the properties of the solvent used for the reaction. Such properties are its dielectric constant, which determines the strength of the solvent cage, its donicity, which reflects the ability of the solvent to establish an H bridge with benzyl radical **12** or with the OH radical (for the formation of H bridges with OH see ref 52), or its possibility to transfer H atoms to one or both radicals captured in the solvent cage. For different solvents, each factor plays a different role.

(1) CCl_3F. Since the solvent does not possess any H atoms, H abstraction is not possible in the solvent cage. There are two possibilities that should lead to an increase of the yield of **7** with increasing temperature: (a) Formation of the ketone **4b** occurs at lower temperature, at which OH production is slow. With increasing temperature the OH production and the formation of **7** increases. (b) The solvent cage encloses both **12** and OH, in which the latter has a finite lifetime before it can leave

(52) Wrobel, R.; Sander, W.; Kraka, E.; Cremer, D. *J. Phys. Chem. A* **1999**, *103*, 3693−3705.

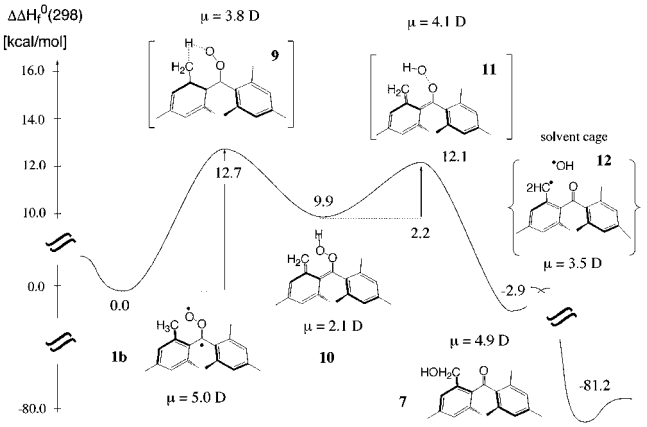

Figure 7. Energy diagram for the formation of alcohol **7**. Relative enthalpies of formation and dipole moments calculated at the B3LYP/6-31G(d) level of theory.

Table 3. Geometrical Parameters of the Mesityl Rings Calculated at B3LYP/6-31G(d)[a]

	ϕ	A	B	(A − B)	σ_A	σ_B
1b	90.3	1.404	1.405	0.001	0.010	0.014
9, TS	86.7	1.418	1.403	0.015	0.039	0.010
10	84.7	1.430	1.404	0.026	0.057	0.010
11, TS	92.7	1.424	1.402	0.022	0.045	0.006
12	87.5	1.412	1.404	0.008	0.021	0.010
7	85.7	1.404	1.404	0.000	0.010	0.010

[a] ϕ denotes the angle (deg) between the normal vectors of rings A and B; averaged CC bond lengths (Å) in rings A and B are listed under the heading A and B, A − B denotes the difference (Å) between average CC bond lengths, σ (Å) gives the standard deviation of CC ring bond lengths from average values for rings A and B.

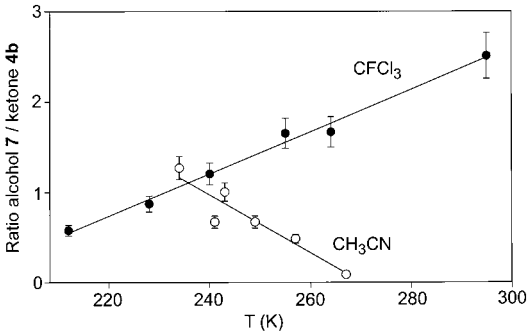

Figure 8. Ratio [alcohol **7**]/[ketone **4b**] as a function of temperature and solvent. (○) acetonitrile; (●) CCl_3F.

in a diffusion process and abstract outside the cage an H atom from traces of dimesitylmethane or other H-containing molecules. With increasing temperature, the movements of the OH radical in the solvent cage become larger, thus increasing the chance to collide with radical **12** in such a way that a new CO bond can be established. In view of the few H-donors in solution, the OH group may even leave and reenter the solvent cage to have a second chance for a reaction with **12**. In any case the yield of alcohol **7** will increase with temperature.

(2) Hexane. In a hexane solvent cage the situation will be first similar to that in the CCl_3F solvent cage, that is, with increasing temperature more alcohol **7** will be formed. However, the solvent participates now in the reaction because it can donate H atoms, provided the temperature is high enough for the H abstraction reaction. Obviously, for T > 240 K this the case, which means that for a further increase in temperature, radical **12** reacts increasingly with the solvent thus raising the yield of ketone **4b**.

(3) Acetonitrile. This solvent forms a stronger solvent cage because of its larger dielectric constant $\epsilon = 36.6$ and, in addition, it is able to establish a H bond with the OH radical. At low temperature the situation should be similar to that in CCl_3F or hexane, that is, an increase of the ratio **7**/**4b** with increasing temperature has to be expected. However, due to the high melting point of CH_3CN the measurements can only be started at 235 K, where the temperature dependence is already reversed. With increasing temperature acetonitrile molecules collide with OH in the cage, form a H bond, and prevent in this way the reaction of OH with radical **12**. Actually, acetonitrile can pull the OH radical out of the cage, thus increasing the yield of ketone **4b**. Once OH is trapped in a solvent cage of its own, it will not have a chance to reenter the solvent cage of **11**.

Conclusions

(1) For the first time it has been possible to investigate a carbonyl oxide by NMR spectroscopy and to determine its conformation by comparing measured and calculated NMR chemical shifts. Experimentally, the average NMR chemical shifts of two enantiomers are measured, and with this in consideration an excellent agreement between measured and calculated shift data is obtained. From that we conclude that the calculated geometry (Figure 2) provides a reliable account of the geometry of **1b**. The ring planes of the two mesityl groups enclose an angle of 90°, which implies a strong steric shielding of the COO unit by the neighboring *ortho*-methyl groups.

(2) Libration of ring B is fast because the calculated barrier is just 3.3 kcal/mol ($\Delta\Delta H_f^0(298) = 3.0$ kcal/mol at B3LYP/6-31G(d)) while libration of ring A is slow on the NMR time scale bacause of a barrier of 15.6 kcal/mol.

(3) We were able to confirm H migration in a carbonyl oxide followed by OH production in solution phase. Carbonyl oxide **1b** rearranges to hydroperoxide **10** (9.9 kcal/mol above **1b**), which is rather labile in view of an activation enthalpy of just 2.2 kcal/mol for OO bond cleavage. The two radicals **12** and OH are formed, which in the gas phase should separate and undergo secondary reactions (H atom abstraction).

(4) The activation enthalpy for H migration is just 12.7 kcal/mol and, by this, 5 kcal/mol lower than the activation enthalpy for the isomerization to dioxirane. In the solution phase, there will be a small increase of the barrier for H migration, but both in the gas phase and in solution phase carbonyl oxide **1b** should exclusively produce OH radicals. We note that the measured activation enthalpy of 13.2 kcal/mol in CCl_3F and of 12.5 kcal/mol in acetonitrile excellently agree with the calculated value.

(5) The formation of either ketone **4b** or alcohol **7** is determined at the stage of the products **12** + OH, embedded in a solvent cage (apart from ketone formed in a side reaction). According to our calculations there is no indication that **7** is formed directly from **10** by an intramolecular concerted reaction. The product ratio **4b:7** depends on the lifetime of OH in the solvent cage. The influence of various solvents on the yield of alcohol **7** can be rationalized.

We conclude that, depending on the structure of a carbonyl oxide (existence of *syn*-positioned substituents with H atoms prone to migrate) and the lifetime of a carbonyl oxide in solution, one has to consider both the possibility of its isomerization to dioxirane and that of OH production yielding either a ketone or an alcohol. In the case of *syn*-alkyl or -aryl substituent with a transferable H atom, OH production seems to be the preferred process irrespective of the environment.

Molecule **1b** is the first carbonyl oxide in solution, for which a detailed study of these two reaction modes is possible and

for which, similar as in the case of dimethyl carbonyl oxide,[33] the OH production route is more favorable. In view of this result, it may be rewarding to analyze previous publications on carbonyl oxides in solution and to check whether the reaction products in line with OH production were found.

Experimental Section

General Methods. NMR spectra were recorded on a Bruker model DRX-400 spectrometer at room temperature and at 200 K. Chemical shifts (δ, ppm) are relative to TMS (^{1}H and ^{13}C). Matrix isolation experiments were performed by standard techniques with an APD DE−204SL and an APD DE−202 Displex closed-cycle helium cryostat. Matrices were produced by deposition of argon on top of a CsI (IR) or sapphire (UV−vis) window with a rate of approximately 0.15 mmol/min. The dimesityldiazomethane was heated in an aluminum tube up to 60 °C. To obtain optically clear matrices the spectroscopic window was retained at 30 K during deposition, and the matrix was subsequently cooled to 10 K. IR-spectra were recorded on a Bruker IFS66 FTIR spectrometer with a standard resolution of 1 to 0.5 cm^{-1} in the range of 400−4000 cm^{-1}.

Irradiations for NMR and thermal decay studies were carried out with use of Osram HBO 500 W/2 or Ushio USH-508SA mercury high-pressure arc lamps in Oriel housing equipped with quartz optics and water filters to remove IR irradiation. For broad-band irradiation Schott cutoff filters were used (50% transmission at the wavelength specified). For narrow-band irradiation interference filters in combination with dichroic mirror ("cold mirror") were used.

Kinetic studies at variable temperature were performed by irradiation of 2.5 × 10^{-5} m solutions of **2b** with a frequency tripled Nd:Yag laser (Coherent Infinity) in combination with an OPO system at 515 nm (repetition rate 50 Hz, 500 mJ/pulse, ca. 20 s irradiation time). The temperature was controlled in the range between 77 K and room temperature using an Oxford Instruments DN1714 liquid nitrogen cryostat with an ITC4 (Oxford Instruments) temperature controller. UV−vis spectra were recorded on a Hewlett-Packard 8452A diode array spectrophotometer with a resolution of 2 nm. For kinetic data every 0.1 s data were collected.

The ratio of alcohol **7** and ketone **4b** was determined with a Siemens GC (Sicromat 1-4) and a 30 m OV1 column, ∅ 0.1 mm at 80 °C. The injection was splitted 1:100 at 200 °C, and detection was carried out with an FID at 200 °C. The sensitizer/solvent combinations were: CCl_3F/5,10,15,20-tetrakis-(pentaflourophenyl)21*H*,23*H*-porphyrin, THF/rose bengal and (pentane/toluene)/C_{60}.

Materials. Argon of high purity (99.9999%, Messer-Griesheim) was used for the matrix isolation experiments. CCl_3F (Merck-Schuchardt), acetonitrile (spectroscopic grade, Acros), hexane (spectroscopic grade, T. J. Baker), and $(CF_2Br)_2$ (ABCR) were dried over molecular sieves 4 Å before use. Rose bengal was purchased from Acros and C_{60} from Riedel-de Haën.

Dimesityldiazomethane (2b). 2b was synthesized by the general route of Zimmermann and Paskovich.[24]

Dimesitylketone *O*-Oxide (1b). For NMR studies dimesityldiazomethane **2b** (3 mg, 1.1 10^{-2} mmol) was dissolved in 0.8 mL of a 1:1 mixture of CCl_3F and $(CF_2Br)_2$ in a NMR tube and bubbled 30 min with oxygen. Afterward the NMR tube was cooled to 77 K, and the organic glass was photolyzed with $\lambda > 515$ nm for 4 h.

For thermal decay studies dimesityldiazomethane **2b** (50 mg, 0.18 mmol) was dissolved in 50 mL of solvent. The solution was cooled with a cryostat, saturated with oxygen, and irradiated with $\lambda > 515$ nm for 5 h. After the solution was colorless, it was warmed to room temperature.

For kinetic measurements dimesityldiazomethane **2b** (6 mg, 2.2 10^{-2} mmol) was dissolved in 5 mL of solvent, cooled to detection temperature, saturated with oxygen, and irradiated with $\lambda = 515$ nm (pulsed laser) for 20 s.

In organic glasses dimesityldiazomethane **2b** (3 mg, 1.1 10^{-2} mmol) was dissolved in 4.2 mL of a 1:1 mixture of CCl_3F and $(CF_2Br)_2$ and saturated with oxygen. After cooling to 77 K, the glass was irradiated with $\lambda > 515$ nm for 4 h.

Quantum Chemical Calculations

Restricted and unrestricted Kohn−Sham theory[53] was applied employing the B3LYP hybrid functional[47,48] in connection with Pople's 6-31G(d) basis set.[49] For all molecules and transition states considered, vibrational frequencies at optimized geometries were determined to characterize stationary points. This was particularly important for finding minima due to the very shallow potentials for methyl group rotations. Zero-point energy (ZPE) and thermal corrections were used to obtain reaction and activation enthalpies $\Delta\Delta H$ at 298 K. The determination of entropies led to free enthalpies ΔG at 298 K.

Calculated energies were refined by carrying out B3LYP single-point calculations with Dunning's cc-pVTZ basis,[50] [new-1] which corresponds to a (11s6p3d2f/6s3p2d) [5s4p3d1f/4s3p2d] contraction and leads to calculations with 938 basis functions in the case of **1b** and its isomers.

The orientation of rings A and B with regard to each other were calculated by determining first the geometrical center and mean plane[54] of each ring, then the normal to each mean plane, and finally, the angle ϕ enclosed by the two normal vectors. NMR chemical shifts were calculated using the IGLO-DFT method by Olsson and Cremer.[55,56] Contrary to the energy calculations, the chemical shift calculations were carried out by employing Becke exchange[57] in connection with the PW91 correlation functional[58] because BPW91 is known to lead to somewhat better shift values.[55,56] As appropriate basis set the (9s5p1d/5s1p) [5s4p1d/3s1p] set of Kutzelnigg and co-workers[59] was employed, which is of VTZ+P quality and which was designed for NMR chemical shift calculations with the IGLO method. As suitable reference TMS was chosen (σ (^{13}C) = 186.07 ppm; σ (^{1}H) = 31.18 ppm calculated at a PW91/[5s4p1d/3s1p] geometry). Calculations were carried out with the program packages COLOGNE2000[60] and GAUSSIAN98.[61]

Acknowledgment. This paper is dedicated to Professor Frank-Gerrit Klärner on the occasion of his 60th birthday. This work was financially supported at Bochum University by the Deutsche Forschungsgemeinschaft (Schwerpunktprogramm Peroxidchemie) and the Fonds der Chemischen Industrie, at Göteborg University by the Swedish Natural Science Research Council (NFR). We thank Professor Henning, University of Leipzig, for providing us with the fluorinated porphyrin. Cray Inc. is kindly acknowledged for providing computational resources to carry out a considerable number of the calculations. Calculations were also done on the supercomputers of the Nationellt Superdatorcentrum (NSC), Linköping, Sweden. E.K. and D.C. thank the NSC for a generous allotment of computer time.

JA003533G

(53) Kohn, W.; Sham, L. J. *Phys. Rev. A* **1965**, *140*, 1133.
(54) Cremer, D.; Pople, J. A. *J. Am. Chem. Soc.* **1975**, *97*, 1354−1358.
(55) Olsson, L.; Cremer, D. *J. Chem. Phys.* **1996**, *105*, 8995−9006.
(56) Olsson, L.; Cremer, D. *J. Phys. Chem.* **1996**, *100*, 16881.
(57) Becke, A. D. *Phys. Rev. A*: *Gen. Phys.* **1988**, *38*, 3098−3100.
(58) Perdew, J. P.; Wang, Y. *Phys. Rev. B* **1992**, *45*, 13244.
(59) Kutzelnigg, W.; Fleischer, U.; Schindler, M. In *NMR, Basic Principles and Progress*; P. Diehl, Ed.; Springer: Berlin, 1991; Vol. 23, p 165.
(60) Kraka, E.; Gräfenstein, J.; Gauss, J.; He, Y.; Reichel, F.; Olsson, L.; Konkoli, Z.; He, Z.; Cremer, D. *COLOGNE2000*; Göteborg University: Göteborg, 2000.
(61) Frisch, M. J.; Trucks, G. W.; Schlegel, H. B.; Scuseria, G. E.; Robb, M. A.; Cheeseman, J. R.; Zakrzewski, V. G.; Montgomery, J. A., Jr.; Stratmann, R. E.; Burant, J. C.; Dapprich, S.; Millam, J. M.; Daniels, A. D.; Kudin, K. N.; Strain, M. C.; Farkas, O.; Tomasi, J.; Barone, V.; Cossi, M.; Cammi, R.; Mennucci, B.; Pomelli, C.; Adamo, C.; Clifford, S.; Ochterski, J.; Petersson, G. A.; Ayala, P. Y.; Cui, Q.; Morokuma, K.; Malick, D. K.; Rabuck, A. D.; Raghavachari, K.; Foresman, J. B.; Cioslowski, J.; Ortiz, J. V.; Stefanov, B. B.; Liu, G.; Liashenko, A.; Piskorz, P.; Komaromi, I.; Gomperts, R.; Martin, R. L.; Fox, D. J.; Keith, T.; Al-Laham, M. A.; Peng, C. Y.; Nanayakkara, A.; Gonzalez, C.; Challacombe, M.; Gill, P. M. W.; Johnson, B.; Chen, W.; Wong, M. W.; Andres, J. L.; Gonzalez, C.; Head-Gordon, M.; Replogle, E. S.; Pople, J. A. *Gaussian 98*, revision A.3; Gaussian, Inc,: Pittsburgh, PA, 1998.